Background Heterogeneity and Other Uncertainties in Estimating Urban Methane Flux: Results from the Indianapolis Flux (INFLUX) Experiment

Nikolay V. Balashov[1*,2,3], Kenneth J. Davis[1], Natasha L. Miles[1], Thomas Lauvaux[1,4], Scott J. Richardson[1], Zachary R. Barkley[1], Timothy A. Bonin[5, 6]

[1]The Pennsylvania State University, University Park, Pennsylvania, USA
[2]NASA Postdoctoral Program, Universities Space Research Association, 7178 Columbia Gateway Drive, Columbia, MD, 21046, USA
[3]NASA Global Modeling and Assimilation Office (GMAO), Goddard Space Flight Center, Greenbelt, MD, 20771, USA
[4]Laboratory of Climate Sciences and Environment, Gif-sur-Yvette, France
[5]Cooperative Institute for Research in Environmental Sciences, Boulder, Colorado, USA
[6]Chemical Sciences Division, National Oceanic and Atmospheric Administration, Boulder, Colorado, USA
[*]Former affiliation

Correspondence to: Nikolay V. Balashov (nvb5011@psu.edu or nikolay.v.balashov@nasa.gov) and Kenneth J. Davis (kjd10@psu.edu)

Abstract

As natural gas extraction and use continues to increase, the need to quantify emissions of methane (CH_4), a powerful greenhouse gas, has grown. Large discrepancies in Indianapolis CH_4 emissions have been observed when comparing inventory, aircraft mass-balance, and tower inverse modeling estimates. Four years of continuous CH_4 mole fraction observations from a network of nine towers as a part of the Indianapolis Flux Experiment (INFLUX) are utilized to investigate four possible reasons for the abovementioned inconsistencies: (1) differences in definition of the city domain, (2) a highly temporally variable and spatially non-uniform CH_4 background, (3) temporal variability in CH_4 emissions, and (4) CH_4 sources that are not accounted for in the inventory. Reducing the Indianapolis urban domain size to be consistent with the inventory domain size decreases the CH_4 emission estimation of the inverse modeling methodology by about 35%, thereby lessening the discrepancy and bringing total city flux within the error range of one of the two inventories. Nevertheless, the inverse modeling estimate still

remains about 91% higher than inventory estimates. Hourly urban background CH_4 mole fractions are shown to be spatially heterogeneous and temporally variable. Variability in background mole fractions observed at any given moment and a single location could be up to about 50 ppb depending on a wind direction, but decreases substantially when averaged over multiple days. Statistically significant, long-term biases in background mole fractions of 2-5 ppb are found from single point observations for most wind directions. Boundary layer budget estimates suggest that Indianapolis CH_4 emissions did not change significantly when comparing 2014 to 2016. However, it appears that CH_4 emissions may follow a diurnal cycle with daytime emissions (12-16 LST) approximately twice as large as nighttime emissions (20-5 LST). We found no evidence for large CH_4 point sources that are otherwise missing from the inventories. The data from the towers confirm that the strongest CH_4 source in Indianapolis is South Side Landfill. Leaks from the natural gas distribution system that were detected with the tower network appeared localized and non-permanent. Our simple atmospheric budget analyses estimate the magnitude of the diffuse NG source to be 70% higher than inventory estimates, but more comprehensive analyses are needed. Long-term averaging, spatially-extensive upwind mole fraction observations, mesoscale atmospheric modeling of the regional emissions environment, and careful treatment of the times of day are recommended for precise and accurate quantification of urban CH_4 emissions.

1 Introduction

From the beginning of the Industrial Revolution to 2011, atmospheric methane (CH_4) mole fractions increased by a factor of 2.5 due to anthropogenic processes such as fossil fuel production, waste management, and agricultural activities (Ciais et al., 2013; Hmiel et al., 2020).

The increase in CH_4 is a concern as it is a potent greenhouse gas (GHG) with a global warming potential 28-34 times greater than that of CO_2 over a period of 100 years (Myhre et al., 2013). The magnitudes of component CH_4 sources, and the causes of variability in the global CH_4 budget are not well understood with theories attributing changes in biogenic, thermogenic, and pyrogenic emissions or a decline in the atmospheric CH_4 sink to the recent CH_4 increases (Nisbet et al., 2016; Saunois et al., 2016; Nisbet et al., 2019; Hmiel et al., 2020). Improved understanding of CH_4 emissions is needed (National Academies of Sciences and Medicine, 2018).

In particular, the estimates of continental U.S. anthropogenic CH_4 emissions disagree. Inventories from Environment Protection Agency (EPA) and Emissions Database for Global Atmospheric Research (EDGAR) in 2008 reported emission values of 19.6 and 22.1 TgC y^{-1} (U.S. EPA, 2013; European Commission Joint Research Centre and Netherlands Environmental Assessment Agency, 2010). However, top-down methodologies using aircraft and inverse modeling framework found emission values of 32.4 ± 4.5 TgC y^{-1} for 2004 and 33.4 ± 1.4 TgC y^{-1} for 2007-2008 respectively (Kort et al., 2008; Miller et al., 2013). Underestimation of natural gas (NG) production and agricultural sources are possible reasons for this disagreement (Miller et al., 2013; Brandt et al., 2014; Jeong et al., 2014). Efforts to reconcile GHGs emissions estimates using atmospheric methods and inventory assessment have sometimes succeeded (Schuh et al., 2013; Zavala-Araiza et al., 2015; Turnbull et al., 2019) when careful attention is given to the details of each method, and targeted atmospheric data are available. A recent synthesis of emissions from the U.S. NG supply chain demonstrated similar success and concluded that current inventory estimates of emissions from U.S. NG production are too low

78 and that emission from NG distribution is one of the greatest remaining sources of uncertainty in
79 the NG supply chain (Alvarez et al., 2018).

80 Due to the uncertainties in CH_4 emissions from NG distribution it is natural that urban
81 emissions are of interest as well. For example, two studies (McKain et al., 2015; Hendrick et al.,
82 2016) indicate that ~60-100% of Boston CH_4 emissions are attributable to the NG distribution
83 system. Recent studies of urban CH_4 emissions in California indicate that the California Air
84 Resources Board (CARB) inventory tends to underestimate the actual CH_4 urban fluxes possibly
85 due to fugitive emissions from NG infrastructures in urban environments (Wunch et al., 2009;
86 Jeong et al., 2016; Jeong et al., 2017). The accuracy and precision of atmospheric estimates of
87 urban CH_4 emissions are limited by available atmospheric observations (Townsend-Small et al.,
88 2012), potential source magnitude variability with time (Jackson et al., 2014; Lamb et al., 2016),
89 errors in atmospheric transport modeling (Hendrick et al., 2016; Deng et al., 2017; Sarmiento et
90 al., 2017), and complexity in atmospheric background conditions (Cambaliza et al., 2014; Karion
91 et al., 2015; Heimburger et al., 2017). In this work, detailed analysis of urban CH_4 mole
92 fractions is performed for the city of Indianapolis to better understand the aforementioned
93 uncertainties of urban CH_4 emissions.

94 The Indianapolis Flux Experiment (INFLUX; Davis et al., 2017) is a testbed for
95 improving quantification of urban GHGs emissions and their variability in space and time.
96 INFLUX (http://influx.psu.edu) is located in Indianapolis partly because of its isolation from
97 other urban centers and the flat Midwestern terrain. It includes a very dense GHGs monitoring
98 network, comprised of irregular insitu aircraft measurements (Heimburger et al., 2017;
99 Cambaliza et al., 2014), continuous in situ observations from communications towers using
100 cavity ring-down spectroscopy (Richardson et al., 2017; Miles et al., 2017), and automated flask

101 sampling systems for quantification of a wide variety of trace gases (Turnbull et al., 2015).
102 Meteorological sensors include a Doppler lidar providing continuous boundary layer depth and
103 wind profiles, and tower-based eddy covariance measurements of the fluxes of momentum,
104 sensible and latent heat (Sarmiento et al., 2017). The network is designed for emissions
105 quantification using top-down methods such as tower-based inverse modeling (Lauvaux et al.,
106 2016) and aircraft mass balance estimates (Cambaliza et al., 2015).

107 Lamb et al. (2016) compared Indianapolis CH_4 emissions estimates from a variety of
108 approaches, specifically inventory, aircraft mass balances, and inverse modeling. The results
109 revealed large mean differences among the city fluxes estimated from these methods (Fig. 1). In
110 general, the inventory methods arrived at lower estimates of emissions compared to the
111 atmospheric, or top-down approaches. CH_4 fluxes calculated using the aircraft mass balance
112 technique varied considerably between flights, more than would be expected from propagation of
113 errors of the component measurements (Cambaliza et al., 2014; Lamb et al., 2016). The
114 atmospheric inverse estimate was significantly higher than the inventory and some of the
115 aircraft-derived values.

116 Biogenic emissions from the city are dominated by a landfill close to downtown, and
117 these emissions are thought to be fairly well known (GHG reporting program). Although
118 evidence of possible variability in landfill emissions exists from Cambaliza et al. (2015), which
119 used aircraft mass balance on five different occasions to calculate CH_4 flux from this landfill.
120 Uncertainty in total city emissions is mainly driven by the uncertainty in thermogenic emissions,
121 which are hypothesized to emerge largely from the NG distribution system (Mays et al., 2009;
122 Cambaliza et al., 2015; Lamb et al., 2016). In this study, we explore potential explanations for

123 the discrepancies in CH_4 emissions estimates from Indianapolis and posit methods and
124 recommendations for the study of CH_4 emissions from other urban centers.

125 We examine four different potential explanations for the CH_4 flux discrepancies reported
126 in Lamb et al. (2016): (1) inconsistent geographic boundaries between top-down and bottom-up
127 studies, (2) heterogeneity in the urban scale CH_4 background and (3) temporal variability in
128 urban emissions, which is not captured by the existing top-down studies, and (4) CH_4 sources
129 that are not accounted for in the inventories. Well-calibrated CH_4 sensors on the INFLUX tower
130 network (Miles et al., 2017) collected continuous CH_4 observations from 2013 to 2016 and
131 provide a unique opportunity to explore these issues.

132

133 **2 Methods**

134

135 **2.1 Experimental site**

136 This study uses data from a tower-based GHG observational network located in the city and
137 surrounding suburbs of Indianapolis, Indiana in the Midwestern U.S. Prior studies have used
138 varying definitions for the region of Indianapolis (Cambaliza et al., 2015; Lamb et al., 2016). In
139 this work, we follow Gurney et al. (2012) and define Indianapolis as the area of Marion County.
140 The flat terrain of the region simplifies interpretation of the atmospheric transport. The land-
141 surface heterogeneity inherent in the urban environment (building roughness, spatial variations in
142 the surface energy balance) does have a modest influence on the wind and boundary layer depth
143 within the city compared to nearby rural areas (Sarmiento et al., 2017).

144 Figure 2 shows two domains that have been used for the evaluation of Indianapolis CH_4
145 emissions (Lamb et al., 2016; Lauvaux et al., 2016). The first domain is the whole area shown in

146 the figure enclosing both Indianapolis and places that lie outside of its boundaries. This domain
147 was used for the inversion performed in Lamb et al. (2016). The second domain is Marion
148 County outlined with a green dashed line. It is assumed here that this domain is much more
149 representative of the actual Indianapolis municipal boundaries as this area encompasses the
150 majority of the urban development associated with the city of Indianapolis (Gurney et al., 2012).
151 The larger domain has three additional landfills that, based on the EPA gridded inventory
152 (Maasakkers et al., 2016), increase Indianapolis CH_4 emissions by about 50% when compared to
153 the smaller domain. The inversion explained in Lamb et al. (2016) has been rerun for two of the
154 domains mentioned above and the results (Fig. 1) have been reexamined.
155
156 **2.2 INFLUX tower network**
157 The continuous GHG measurements from INFLUX are described in detail in Richardson et al.
158 (2017). The measurements were made using wavelength-scanned cavity ring down
159 spectrometers (CRDS, Picarro, Inc., models G2301, G2302, G2401, and G1301), installed at the
160 base of existing communications towers, with sampling tubes secured as high as possible on each
161 tower (39 – 136 m above ground level (AGL); Miles et al., 2017). A few towers also included
162 measurements at 10 m AGL and one or two intermediate levels. While INFLUX tower in-situ
163 measurements began in September 2010, here we focus on the CH_4 measurements from 2013 –
164 2016. From June through December 2012, there were two or three towers with operational CH_4
165 measurements. By July 2013, five towers included measurements of CH_4, and throughout the
166 majority of the years 2015 – 2016 there were eight INFLUX towers with CH_4 measurements
167 (Fig. 3). Flask to in-situ comparisons and round-robin style testing indicated compatibility

168 across the tower network of 0.6 ppb CH_4 (Richardson et al., 2017). In this study we use hourly
169 means of CH_4.
170
171 **2.3 Meteorological data**
172 Wind speed and direction were measured at the Indianapolis International Airport (KIND), Eagle
173 Creek Airpark (KEYE), and Shelbyville Municipal Airport (KGEZ). The data used are hourly
174 values from the Integrated Surface Dataset (ISD) (https://www.ncdc.noaa.gov/isd) and 5-minute
175 values directly from the Automated Surface Observing System (ASOS). A complete description
176 of ASOS stations is available at https://www.weather.gov/media/asos/aum-toc.pdf. The
177 accuracy of the wind speed measurements are ±1 m/s or 5% (whichever is greater) and the
178 accuracy of the wind direction is 5 degrees when the wind speed is ≥ 2.6 m/s. The anemometers
179 are located at about 10 meters AGL. The wind data reported in ISD are given for a single point
180 in time recorded within the last 10 minutes of an hour and are closest to the value at the top of
181 the hour.
182 The planetary boundary layer height (BLH) was determined from a Doppler lidar
183 deployed in Lawrence, Indiana about 15 km to the northeast of downtown. The lidar is a Halo
184 Streamline unit, which was upgraded to have extended range capabilities in January 2016. The
185 lidar continuously performs a sequence of conical, vertical-slice, and staring scans to measure
186 profiles of the mean wind, turbulence, and relative aerosol backscatter. All of these
187 measurements are combined using a fuzzy-logic technique to automatically determine the BLH
188 continuously every 20-min (Bonin et al., 2018). The BLH is primarily determined from the
189 turbulence measurements, but the wind and aerosol profiles are also used to refine the BLH
190 estimate. The BLHs are assigned quality-control flags that can be used to identify times when

191 the determined BLH is unreliable, such as when the air is exceptionally clean, the BLH is below
192 a minimum detectable height, or clouds and fog that attenuate the lidar signal exist. Additional
193 details about the algorithm and the lidar operation for the INFLUX project are provided in Bonin
194 et al. (2018). Doppler lidar measurements are available at
195 https://www.esrl.noaa.gov/csd/projects/influx/.
196
197 **2.4 Urban methane background**
198 Both aircraft mass balance and inverse modeling methodologies rely on an accurate estimation of
199 the urban CH_4 enhancement relative to the urban CH_4 background in order to produce a reliable
200 flux estimate (Cambaliza et al., 2014; Lamb et al., 2016). The CH_4 mole fraction enhancement is
201 defined as,

$$C_{enhancement} = C_{downwind} - C_{bg} \quad (1)$$

202 where $C_{downwind}$ is the CH_4 mole fraction measured downwind of a source and C_{bg} is the CH_4
203 background mole fraction, which can be measured upwind of the source, but this is not
204 necessary. Background, as defined in this body of literature, is a mole fraction measurement that
205 does not contain the influence of the source of interest, but which is assumed to accurately
206 represent mole fractions that are upwind of the source of interest and measured simultaneously
207 with the downwind mole fractions.
208 Aircraft mass balance studies of Indianapolis mentioned used two main methods to
209 determine a background value. The first method calculates an average of the aircraft transect
210 edges that lie outside of the city domain (Cambaliza et al., 2014). In the second approach, a
211 horizontally varying background is introduced by linearly interpolating median background
212 values of each of the transect edges (Heimburger et al., 2017). In theory there is also a third

213 method that uses an upwind transect as a background field, but in the studies above it was
214 assumed that the edges are representative of an upwind flow. In the case of an inversion, it is
215 common to pick a tower that is located generally away from urban sources and has on average
216 the smallest overall enhancement (Lavaux et al., 2016). Because choosing the background
217 involves a degree of subjectivity (Heimburger et al., 2017) we consider how these choices may
218 influence emission estimates and introduce error, both random and systematic, using data from
219 the INFLUX tower network.

220 Using tower network data from November 2014 through the end of 2016, two CH_4
221 background fields are generated for the city of Indianapolis based on two different sets of
222 criteria. The notion is based on the fact that a choice of background is currently rather arbitrary
223 in the literature (Heimburger et al., 2017) and at every point in time it is possible to choose
224 multiple background values that are equally acceptable for the flux estimation. In our case both
225 approaches identify a tower suitable to serve as a background for each of the eight wind
226 directions (N, NE, E, SE, S, SW, W, NW), where an arc of 45° represents a direction (e.g. winds
227 from N are between 337.5° and 22.5°). Estimating background for different wind directions is
228 implemented to more accurately represent upwind flow that is hopefully not contaminated by
229 local sources.

230 Criterion 1 corresponds to a typical choice of a background in a case of tower inversion
231 and is based on the concept that the lowest CH_4 mole fraction measured at any given time is not
232 affected by the city sources and therefore is a viable approximation of the background CH_4 mole
233 fractions outside of the city (Miles et al., 2017; Lauvaux et al., 2016). Given this assumption, the
234 tower with the lowest median of the CH_4 enhancement distribution (calculated by assuming the
235 lowest measurement among all towers at a given hour as a background) for each of the wind

directions over the November 2014 through December 2016 time period is chosen as a background site (Miles et al., 2017). Criterion 2 requires that the tower is outside of Marion County (outside of the city boundaries) and is not downwind of any known regional CH_4 source (Fig. 2). For some wind directions, there are multiple towers that could qualify as a background; we pick towers in such a manner that they are different for each criterion given a wind direction in order to calculate the error associated with the use of different but acceptable backgrounds. The towers used for both criteria and for each of the eight wind directions are displayed in Table 1. Quantifying differences between these two backgrounds allows for an opportunity to better understand the degree of uncertainty that exists in the atmospheric CH_4 background at Indianapolis.

To make the comparison as uniform as possible only data from 12-16 LST are utilized (all hours are inclusive) when the boundary layer is typically well-mixed (Bakwin et al., 1998). A lag 1 autocorrelation is found between 12-16 LST hours, i.e. the hourly afternoon data are correlated to the next hour, but the correlation is not significant for samples separated by two hours or more. Therefore, hours 13 and 15 LST are eliminated to satisfy the independence assumption for hourly samples. Furthermore, we make an assumption that the data satisfy steady state conditions. If the difference between consecutive hourly wind directions exceeds 30 degrees or the difference between hours 16 and 12 LST exceeds 40 degrees, the day is eliminated. Days with average wind speeds below 2 m/s are also eliminated due to slow transport across the city (the transit time from tower 1 to tower 8 is about 7 hours at a wind speed of 2 m/s).

2.5 Frequency and bivariate polar plots

Frequency and bivariate polar plots are used in this work to gain more knowledge regarding CH_4 background variability based on criteria 1 and 2, and to identify sources located within the city. To generate these polar plots, we use the *openair* package (from R programming language) created specifically for air quality data analysis (Carslaw and Ropkins, 2012). Bivariate and frequency polar plots indicate the variability of a pollutant concentration at a receptor (such as an observational tower) as a function of wind speed and wind direction, preferably measured at the location of the receptor or within several kilometers of the receptor. The frequency polar plot is generated by partitioning the CH_4 hourly data into the wind speed and direction bins of 1 m s^{-1} and 10° respectively. To generate bivariate polar plots, wind components u and v are calculated for hourly CH_4 mole fraction values, which are fitted to a surface using a Generalized Additive Model (GAM) framework in the following way,

$$\sqrt{C} = \beta + s(u, v) + \epsilon \quad (2)$$

where C is the CH_4 mole fraction transformed by a square root to improve model diagnostics such as a distribution of residuals, β is mean of the response, s is the isotropic smoothing function of the wind components u and v, and ϵ is the residual. For more details on the model see Carslaw and Beevers (2013).

2.6 Temporal variability and approximate flux estimation

Temporal variability in urban CH_4 emissions may play an important role in the corresponding emissions quantification procedures. Lamb et al. (2016) suggested that such temporal variability might partially explain the differences among CH_4 flux estimates shown in Figure 1. If temporal variability of CH_4 emissions exists within the city, disagreements in the CH_4 flux between studies could be attributed to differences in their sampling period. Because the INFLUX tower

281 data at Indianapolis contain measurements at all hours of the day over multiple years, we can
282 utilize this dataset to better understand the temporal variability in methane emissions in the city.

283 We apply a simplified atmospheric boundary layer budget, not to estimate precisely the
284 actual city emissions, but rather to evaluate temporal variability of the emissions. We begin by
285 assuming CH_4 emissions Q_a (mass per unit time per unit area) are not chemically active and are
286 constant over a distance Δx spanning a significant portion of the city. The next assumption is
287 that a CH_4 plume measured downwind of the city is well mixed within a layer of depth H (which
288 is the same as BLH). We treat wind speed u as constant within the layer for every hour
289 considered. Given the above-mentioned assumptions we can write a continuity equation
290 describing mass conservation of CH_4 concentration C within a box in the following fashion,

$$\Delta x H \frac{\partial C}{\partial t} = \Delta x Q_a + uH(C_b - C) + \Delta x \frac{\partial H}{\partial t}(C_a - C) \quad (3)$$

291 where C_b is the CH_4 concentration upwind of the city (or background), and C_a is the CH_4
292 concentration above the mixed layer (Hanna et al., 1982; Arya, 1999; Hiller et al., 2014). The
293 left hand side of the equation represents the change in CH_4 concentration with time, $\Delta x Q_a$
294 denotes a constant CH_4 source over the distance Δx, $uH(C_b - C)$ indicates a change of CH_4
295 concentration due to horizontal advection, and finally $\Delta x \frac{\partial H}{\partial t}(C_a - C)$ term accounts for the
296 vertical advection and encroachment processes that result from changing BLH. By assuming
297 steady state conditions ($\frac{\partial C}{\partial t} = 0$ and $\frac{\partial H}{\partial t} = 0$), the equation can be simplified to

$$Q_a = \frac{uH(C - C_b)}{\Delta x} \quad (4)$$

298 We use equation 4 to estimate hourly CH_4 emissions (Q_a) from Indianapolis (see
299 assumptions in the paragraph below) given hourly averaged data of H from the lidar positioned
300 in the city, wind speed (u) from the local weather stations, and upwind (C_b) and downwind (C)

301 CH_4 mole fractions measured (and then converted to concentrations) at towers 1, 8, and 13
302 (depending on a wind direction) using data from heights of 40 m, 41 m, and 87 m respectively
303 (see Fig. 2).

304 The CH_4 concentrations are derived from CH_4 mole fractions by approximating average
305 molar density of dry air (in mol m^{-3}) within the boundary layer for every hour of the day, where
306 variability of pressure with altitude is calculated using barometric formula and it is assumed that
307 temperature decreases with altitude by 6.5 K per kilometer. The hourly surface data for pressure
308 and temperature are taken from KIND weather station. The difference between concentrations
309 $C - C_b$ is instantaneous and not lagged, where C_b represents air parcel entering the city and C
310 represents the same air parcel exiting the city (Turnbull et al., 2015). The CH_4 enhancements
311 $C - C_b$ are estimated for daytime by averaging observations spanning 12-16 LST and for
312 nighttime by averaging observations spanning 20-5 LST. These time periods are based on lidar
313 estimations of when on average H varies the least. The day and night were required to contain at
314 least 3 and 9 hourly CH_4 values respectively for averaging to occur, otherwise the day/night is
315 eliminated. Observations when H is below 100 m are not used to avoid the cases when
316 measurements from towers may be above the boundary layer. In order to better achieve the
317 assumption that the boundary layer is fully mixed (especially at night), all hours with wind
318 speeds below 4 m/s are eliminated (Van De Wiel., 2012). To approximate the emissions of the
319 whole city we need to know the approximate area of the city and the distance over which the
320 plume is affected by the city CH_4 sources. The area of the city is about 1024 km^2 (the area of
321 Marion County) and the length that plume traverses when it is over the city ranges from 32 to 35
322 km depending on which downwind tower is used. We assume that CH_4 measurements at towers
323 8 and 13 are representative of a vertically well-mixed city plume as the towers are located

outside of the city boundaries and allow for sufficient vertical mixing to occur. For S and SW wind directions tower 8 observations are used to represent downwind conditions with background observations coming from towers 1 and 13, respectively (based on criterion 1 shown in Table 1). For W wind direction, tower 13 observations represent the downwind with background obtained from tower 1. The wind direction is required to be sustained for at least 2 hours, otherwise the data point is eliminated.

2.7 Indianapolis CH_4 sources

Only a few known CH_4 point sources exist within Indianapolis (Cambaliza et al., 2015; Lamb et al., 2016). The Southside Landfill (SSLF), located near the center of the city, is thought to be the largest point source in the city with emissions ranging between about 28 mol/s (inventory from Maasakkers et al. (2016), GHG reporting program, and inverse estimates from ground-based mobile sampling employed in Lamb et al. (2016)) and 45 mol/s (aircraft; Cambaliza et al. (2015)) depending on an emission estimation methodology. However, using Cambaliza et al. (2015) aircraft data and applying a different background formulation Lamb et al. (2016) found emission values of SSLF closely agreeing with 28 mol/s estimate. SSLF could account for as little as 33% (top-down from Cambaliza et al. (2015)) or as much as 63% (inventory from Maasakkers et al. (2016)) of total Marion County CH_4 emissions. Other city point sources are comparatively small; the wastewater treatment facility located near SSLF contributes about 3-7 mol/s (inventory from Lamb et al. (2016)), and the transmission-distribution transfer station at Panhandle Eastern Pipeline (also known as a city gate and further in this study abbreviated as PEP) is estimated to be about 1 mol/s (inventory from Lamb et al. (2016)). The remaining CH_4 sources, mainly from NG infrastructure leaks and livestock, are considered to be diffuse sources

and are not well known. Potential sources of emissions related to NG activities include gas regulation meters, transmission and storage, distribution leaks, and Compressed Natural Gas (CNG) fleets. These diffuse NG sources account for 21-67% of the city emissions or 20 mol/s (inventory from Maasakkers et al. (2016)) to 64 mol/s (top down from Cambaliza et al. (2015)). Livestock emissions for Marion County are estimated to be around 1.5 mol/s (inventory from Maasakkers et al. (2016)). These prior studies present conflicting conclusions regarding the magnitude of the diffuse NG CH_4 source in Indianapolis.

3 Results and discussion

3.1 Inversion and city boundaries

A significant portion of CH_4 emissions across the U.S. can be characterized by numerous relatively large point sources scattered throughout the country rather than by broad areas of smaller enhancements (Maasakkers et al., 2016). Because of this, the total emissions for a given domain can be very sensitive to how that domain is defined. A small increase or decrease in the domain area could add or remove a large point source and significantly impact the total emissions defined within the domain.

In the case of Indianapolis, this issue became apparent when the emissions were calculated using an atmospheric inversion model (Lamb et al., 2016; Lauvaux et al., 2016). The atmospheric inversion solved for fluxes in domain 1 (Fig. 2), which significantly increased the estimated emissions in comparison with the inventory values that were gathered mainly within Marion County (domain 2). When reduced to domain 2, inverse modeling emission estimate decreases to 107 mol/s (from about 160 mol/s), which falls within an error bar of Lamb et al. (2016) inventory estimate. This difference is significant and could at least partially explain the discrepancy shown in Figure 1 between the emission values from the inventories and emission

results from the inverse modeling. However, even the decreased inverse modeling estimate is about 91% higher than the inventories.

Additionally, the subject of the domain is relevant for airborne mass balance flights because a priori the magnitude and variability of background plume is unknown and could be easily influenced by upwind sources. The issue of background is discussed further in the next section.

3.2 Variability in CH_4 background

Comparisons between criterion 1 and criterion 2 CH_4 background mole fractions as a function of wind speed and direction are visualized using frequency and bivariate polar plots (Fig. 4). Both backgrounds generally agree on the higher CH_4 originating from the SW, SE, and E wind directions (Figs. 4c-f); however, the values themselves differ especially when winds are from NW, SW, and SE. As background difference plots (Figs. 4g-h) indicate, there is a noticeable variability between the magnitudes of the CH_4 backgrounds, where criterion 2, by design, typically has higher background mole fractions. The background differences, at a given hour, suggest that the CH_4 field flowing into the city is heterogeneous with differences between towers ranging from 0 to over 45 ppb (Fig. 4g). Because large gradients in CH_4 background over the city could pose challenges for flux estimations using top down methods such as inverse modeling and aircraft mass balance, it is imperative to establish whether the background differences vary randomly or systematically and how to choose a background to minimize these errors.

To further understand the nature of background variability we calculate the mean, standard deviation, and standard error of background hourly differences between criterion 2 and

criterion 1 from November 2014 to December 2016 for each of the eight wind directions mentioned in Table 1. The results are shown in Figure 5. Systematic bias is evident for the SE, S, SW, W, and NW wind sectors, whereas random error dominates N, NE, and E wind directions. Wind directions showing statistically significant bias have mean biases ranging from 2 to 5 ppb, with values as large as 8 ppb falling within the range of 2 × standard error. Standard deviation plot indicates potential background discrepancy that can occur on any given day, where W wind direction is the least variable with 2 × standard deviation close to 20 ppb, while SE wind direction is the most variable with 2 × standard deviation falling at about 50 ppb.

Random errors in the mole fractions of background differences (biases) are also important and are a function of the length of the data record. We quantify the random error in the CH_4 background mole fraction differences using the bootstrap method by randomly sampling 2 to 150 hours (small and large sample size) of the background CH_4 differences for each of the wind directions with replacement (we make the assumption that our differences are independent since we eliminated lag 1 autocorrelation from the data). This sub-sampling experiment is repeated 5000 times (Efron and Tibshirani, 1986). The standard deviations of the mean (standard error) of the 5000 simulated differences are calculated for each wind direction. The resulting standard errors of the city CH_4 background differences, multiplied by 2 to represent the 95% confidence intervals, are shown as a function of the length of the data record in Figure 6. Because random error falls as sample size grows it makes sense to assign a threshold indicating a minimum number of samples needed to achieve a theoretical precision for each wind direction.

One way to assign a required precision would be to make sure that the standard error (random error) reaches a point where it is less than Indianapolis enhancement of about 12 ppb (a higher estimate of the Indianapolis enhancement from section 3.3) by a factor of 2 when

418 combined with a bias (Table 2). Meaning that the sum of bias and standard error must be at most
419 6 ppb. In this approach each wind direction would have a different threshold because of the
420 differences in biases. For instance, given this requirement NW direction would need a random
421 error of 1 since its bias is 5. For NW direction, this threshold would require more than 150
422 samples. For N direction on the other hand, where the bias is 1, the requirement is fulfilled when
423 random error crosses 5 ppb at 74 samples. Now we consider these random and systematic errors
424 in CH_4 background differences in the context of Indianapolis urban CH_4 emissions.

425 For Indianapolis, using the INFLUX network, we estimated that depending on sample
426 size (number of hours sampled) and wind direction, background gradient across the city over 12-
427 16 LST could vary from 0 to about 50 ppb (Fig. 5b). Given that the average afternoon CH_4
428 enhancement of the city is around 8-12 ppb (section 3.3; Fig. 7; Cambaliza et al., 2015; Miles et
429 al., 2017), the error on the estimated emissions could easily be over 100% if the analysis does not
430 approach the issue of background with enough sampling. A sample size of about 50 independent
431 hours significantly decreases background uncertainty for N, NE, E, S, and W wind directions and
432 allows for a more accurate assessment of the CH_4 emissions at Indianapolis. For CH_4 sources
433 with a significantly larger signal than their regional background, the mentioned background
434 variability becomes less impactful on results, but because Indianapolis is a relatively small
435 emitter of CH_4, and because there are relatively large sources outside of the city, uncertainties
436 due to background estimation are comparatively large. Our uncertainty assessment suggests that
437 the highly variable CH_4 emission values of Indianapolis from aircraft mass balance calculations
438 shown in Figure 1 are at least partially due to the variability in the urban CH_4 background of
439 Indianapolis.
440

441 **3.3. Temporal variability of methane enhancements and fluxes in Indianapolis**

442 Figure 7 presents average CH_4 mole fraction enhancements and flux calculations
443 (equation 4) at towers 8 and 13 for years 2014, 2016, and 2013-2016 (for the detailed
444 methodology see section 2.6). The years of 2014 and 2016 are chosen for temporal comparison
445 because they do not contain major BLH data gaps. The error bars in the figure show the standard
446 error multiplied by 2 indicating 95% confidence interval of each average.

447 One of the more interesting features in Figure 7 is a day/night variability of CH_4
448 emissions at Indianapolis. The most prominent example of this feature is found in Figure 7c,
449 where the estimates for both years suggest that daytime emissions are approximately twice as
450 large as the emissions at night. The decrease of the CH_4 emissions at night also appears in tower
451 13, but the errors are too high in those estimates to make any definitive conclusions. A similar
452 urban CH_4 emissions diurnal variability is reported by Helfter et al. (2016) in their study of
453 GHGs for London, UK, where they attribute diurnal variation of CH_4 emissions to the NG
454 distribution network activities, fugitive emissions from NG appliances, and to temperature-
455 sensitive CH_4 emission sources of biogenic origin (such as a landfill). Taylor et al. (2018)
456 suggest that CH_4 emissions from landfills exhibit a diurnal cycle with higher emissions in early
457 afternoon and 30-40% lower emissions at night.

458 With regard to yearly temporal variability we are only able to compare years 2014 and
459 2016 due to limited BLH data for other years. Results from both towers suggest that
460 Indianapolis overall CH_4 emissions did not change significantly between 2014 and 2016.
461 Although it is important to be cautious about interpreting actual flux estimations given the
462 assumptions mentioned in section 2.6, it is interesting to note that the flux values from both
463 towers average to about 70 mol/s, which puts our value right in between inventory and inversion

estimates shown in Figure 1. If we assume that SSLF emissions are generally known (GHG reporting program) that would indicate that emissions from NG distribution are likely to be about 14 mol/s (70%) higher than what both of the inventories currently estimate but within the error bars of Lamb et al. (2016)'s inventory calculation. Another possible scenario is that SSLF emissions are higher than what is currently assumed. Given these complexities, uncertainty regarding the exact emissions from NG distribution at Indianapolis still remains.

3.4 Methane Sources in Indianapolis

Bottom-up emission inventories have difficulty tracking changes in sources over time. Our continuous tower network observations can monitor temporal and spatial variability in sources of CH_4 in Indianapolis. To do so we employ the aforementioned bivariate polar plots to verify known sources and potentially identify unknown sources across the city. We compare two time periods, 2014-2015 (two full years) and 2016. Figure 8 displays bivariate polar plots of CH_4 enhancements using criterion 1 background at 9 INFLUX towers in Indianapolis over the two years of 2014 and 2015. Figure 9 shows the same plot, but for the year 2016. Here we have separated 2016 from 2014-2015 because of different results noted during these times.

The images reveal that the most consistent and strongest source in the city is the SSLF. This is most evident from the 40+ ppb CH_4 enhancements detected at towers 7, 10 and 11 coming from the location of the SSLF (by triangulation). Enhancements from the landfill appear to also be detectable at towers 2, 4, 5, and 13. Based on these observations it can be concluded that there are no other point sources in Marion County comparable in size to the SSLF. A small fraction of the SSLF plume is likely due to the co-located wastewater facility, but the inventory estimates suggest that the wastewater treatment facility is responsible for no more than 7% of

this plume (Cambaliza et al., 2015; Massakkers et al., 2016). The PEP, located in the northwestern section of the city, may be partially responsible for a plume of 5-10 ppb at towers 5 and 11. However, the plume is less detectable using the criterion 2 background value that has higher background (using tower 8 as a background) from NW wind direction (not shown), adding uncertainty to the true magnitude of the enhancement from this source. The same is true for towers 2 and 13, which have pronounced plumes when winds are from the NW with the criterion 1 background, but when background 2 is used these plumes vanish (not shown). Such inconsistency makes it difficult to attribute these plumes to a specific source.

Another important point is the cluster of large enhancements surrounding tower 10 in 2014-2015. Because no other tower sees these enhancements (at least at comparable magnitudes), we believe that they are the result of nearby NG leaks. These plumes are not consistent temporally or spatially as they mostly disappear in 2016, potentially indicating that they are transient and localized NG distribution leaks. It is difficult to ascertain the exact combined magnitude of these leaks since they mix together with SSLF into an aggregated city plume when observed from downwind towers such as 8 and 13. None of the individual leaks appears to be similar in magnitude to the emissions that originate from SSLF. Diffuse NG emissions comparable to the SSLF source (Lamb et al., 2016) may exist. Our flux estimations at towers 8 and 13, however, imply that the magnitude of NG diffuse source suggested by the top-down analyses in Cambaliza et al. (2015) and Lamb et al. (2016) are probably overestimates (see section 3.3). We hypothesize that the relatively high Indianapolis CH_4 emissions (see Fig. 1) reported by Cambaliza et al. (2015) could be a result of random errors in upwind conditions (see section 3.2) influencing the small number of airborne flux estimates.

4 Conclusions

We have examined four potential contributions to discrepancies between urban top-down and bottom-up estimates of CH_4 emissions from Indianapolis: domain definition, heterogeneous background mole fractions, temporal variability in emissions, and sources missing from inventories. Results indicate that the urban domain definition is crucial for the comparison of the emission estimates among various methods. Our atmospheric inverse flux estimates for Marion County, which is similar to the domain that is analyzed by inventory and airborne mass balance methodologies (Mays et al., 2009; Cambaliza et al., 2014; Lamb et al., 2016), is 107 mol/s compared to 160 mol/s that is estimated for the larger domain (Hestia inventory domain; Gurney et al., 2012). This partially explains higher emissions in inverse modeling estimates shown by Lamb et al. (2016); however, 107 mol/s is still 91% higher than what EPA and Lamb et al. (2016) find in their inventories (Fig. 1).

To better understand background variability at Indianapolis two different but acceptable background estimates, based on specific criteria for each wind direction, and their differences are used to assess heterogeneity of CH_4 background at Indianapolis. Background criterion 1 looks for a tower that is consistently lower than other towers, while background criterion 2 picks a tower that is outside of Marion County domain and is not downwind of any nearby sources as determined by EPA 2012 inventory. We focus on midday atmospheric conditions to avoid the complexities of vertical stratification in the stable boundary layer. The midday Indianapolis atmospheric CH_4 mole fraction background is shown to be heterogeneous with 2-5 ppb statistically significant biases for NW, W, SW, S and SE wind directions. Random errors of background differences are a function of sample size and decrease as a number of independent samples increase. Small sample sizes, such as a few hours of data from a single point, are prone

533 to random errors on the order of 10-30 ppb in the CH_4 background, similar to the magnitude of
534 the total enhancement from the city of Indianapolis, which is estimated to be on average around
535 10-12 ppb. Longer-term sampling and/or more extensive background sampling are necessary to
536 reduce the random errors. Sample size required to reduce random errors of background
537 differences to an acceptable value for flux calculation is largely dependent on a wind direction.
538 Both bias (long-term average of background differences) and its random error are important
539 when estimating total background uncertainty. The results indicate that N, NE, E, S, and W
540 wind directions are more favorable for flux estimation and would require multiple days of
541 measurements (e.g. about 50 independent hours of measurements) to reduce background
542 uncertainty to about 6 ppb, which is half the magnitude of the typical CH_4 enhancement from
543 Indianapolis. The remaining wind directions would require over 150 independent hourly
544 measurements to achieve similar precision. We also estimate that depending on a wind direction
545 for any given hour the spatial variability in background can be anywhere from 0 to 50 ppb. This
546 uncertainty in the CH_4 background may partially explain Heimburger et al. (2017) finding of
547 large variability in airborne estimates of Indianapolis CH_4 emissions. Given many samples, the
548 airborne studies converge to an average value of CH_4 flux that is noticeably closer to the
549 inventory estimates for Indianapolis than several of the individual estimates presented in Figure
550 1.

551 Measurement and analysis strategies can minimize the impacts of these sources of error.
552 Spatially extensive measurement of upwind CH_4 mole fractions are recommended. For towers or
553 other point-based measurements, multiple upwind measurement locations are clearly beneficial.
554 For the aircraft mass balance approach, we recommend an upwind transect to be measured,
555 lagged in time if possible, to provide a more complete understanding of the urban background

556 conditions. Complex background conditions might suggest that data from certain days or wind
557 directions should not be used for flux calculation. Finally, a mesoscale atmospheric modeling
558 system informed with the locations of important upwind CH_4 sources can serve as a powerful
559 complement to the atmospheric data (Barkley et al., 2017). Such simulations can guide sampling
560 strategies, and aid in interpretation of data collected with moderately complex background
561 conditions.

562 With regard to temporal variability, no statistically detectable changes in the emission
563 rates were observed when comparing 2014 and 2016 CH_4 emissions. However, a large
564 difference between day and night CH_4 emissions was implied from a simple budget estimate.
565 Night (20-5 LST) emissions may be 2 times lower than the emissions during the afternoon (12-
566 16 LST) hours. Because prior estimates of top-down citywide emissions are derived using
567 afternoon-only measurements, overall emissions of Indianapolis may be lower than these studies
568 suggest. This bias may be present in studies performed in other cities as well. Our study
569 suggests that day/night differences in CH_4 emissions must be understood if regional emission
570 estimates are to be calculated correctly. Long-term, tower-based observations are an effective
571 tool for understanding and quantifying multi-year variability in urban emissions.

572 One final point addressed in this study is the location of major CH_4 sources in
573 Indianapolis. Analysis of the INFLUX tower observations suggest a diffuse NG source that
574 exceeds both of the inventory estimates by 70%, but additionally our analysis shows that the
575 discrepancy is less than that proposed by highest values reported in Lamb et al. (2016) (see Fig.
576 1). Uncertainty remains regarding the magnitude of the diffuse NG source of CH_4. The only
577 major point source in the city is SSLF and it is observed at multiple towers. There is an evidence

578 for occasional point-source NG leaks, but they appear to be transient in time, and limited in their
579 strength.

580 Overall, assessment of the CH_4 emissions at Indianapolis highlights a number of
581 uncertainties that need to be considered in any serious evaluation of urban CH_4 emissions. These
582 uncertainties amplify for Indianapolis since the enhancement signal from its CH_4 emissions is
583 comparable in magnitude to variability in the regional background flow and as our results show
584 it may be difficult at times to distinguish noise in the background from the actual city emissions
585 signal. The evaluation of larger CH_4 sources may be easier with respect to separating signal
586 from background. However, all of the points raised in this work will be nonetheless relevant and
587 need to be addressed for our understanding of urban CH_4 emissions to significantly improve.

588

589 **Author Contribution**

590 Nikolay Balashov, Kenneth Davis, and Natasha Miles developed the study and worked together
591 on generating the main hypothesis of this work. They also wrote most of the manuscript.
592 Nikolay Balashov wrote all of the codes and performed the analyses presented in this work as
593 well as generated all of the figures. Natasha Miles and Scott Richardson helped with
594 maintenance and gathering of the INFLUX tower data. They also wrote section 2.2 of the paper.
595 Thomas Lauvaux helped with the analysis presented in Fig. 1 and section 3.1 concerning
596 interpretation of the inversion modeling results from Lamb et al. (2016). Thomas Lauvaux also
597 helped with repeating the inversion experiment for two different Indianapolis domains (Fig. 1).
598 Zachary Barkley significantly contributed to discussions regarding the hypothesis and careful
599 presentation of sections 2.6 and 3.3. Timothy Bonin provided all of the lidar data and wrote the

second part of section 2.3 regarding the lidar and the methodology used to determine planetary boundary layer heights. He also contributed to sections 2.6 and 3.3.

Competing Interests

The authors declare that they have no conflict of interest.

Acknowledgements

This research has been supported by the National Institute of Standards and Technology (project number 70NANB10H245). We would like to thank Dr. Bram Maasakkers for the helpful discussion regarding the EPA 2012 inventory and the relevant error structure. We also thank Dr. Paul Shepson and Dr. Brian Lamb for their useful input regarding airborne mass balance flights and the process of compiling an emissions inventory. Most importantly, we would like to acknowledge significant contributions of both reviewers who rigorously examined our science and noticeably improved clarity of our article.

References

Alvarez, R. A., Zavala-Araiza, D., Lyon, D. R., Allen, D. T., Barkley, Z. R., Brandt, A. R., Davis, K. J., Herndon, S. C., Jacob, D. J., Karion, A., Kort, E. A., Lamb, B. K., Lauvaux, T., Maasakkers, J. D., Marchese, A. J., Omara, M., Pacala, S. W., Peischl, J., Robinson, A. L., Shepson, P. B., Sweeney, C., Townsend-Small, A., Wofsy, S. C., and Hamburg, S. P.: Assessment of methane emissions from the U.S. oil and gas supply chain, Science, 10.1126/science.aar7204, 2018.

Arya, S. P.: Air pollution meteorology and dispersion, Oxford University Press New York, 1999.

Barkley, Z. R., Lauvaux, T., Davis, K. J., Deng, A., Miles, N. L., Richardson, S. J., Cao, Y., Sweeney, C., Karion, A., Smith, M., Kort, E. A., Schwietzke, S., Murphy, T., Cervone, G., Martins, D., and Maasakkers, J. D.: Quantifying methane emissions from natural gas

production in north-eastern Pennsylvania, Atmos. Chem. Phys., 17, 13941-13966, 10.5194/acp-17-13941-2017, 2017.

Bakwin, P. S., Tans, P. P., Hurst, D. F., and Zhao, C.: Measurements of carbon dioxide on very tall towers: results of the NOAA/CMDL program, Tellus, 50B, 401–415, 1998.

Bonin, T. A., Carroll, B. J., Hardesty, R. M., Brewer, W. A., Hajny, K., Salmon, O. E., and Shepson, P. B.: Doppler lidar observations of the mixing height in Indianapolis using an automated composite fuzzy logic approach, Journal of Atmospheric and Oceanic Technology, 35, 473-490, 10.1175/jtech-d-17-0159.1, 2018.

Brandt, A. R., Heath, G. A., Kort, E. A., O'Sullivan, F., Pétron, G., Jordaan, S. M., Tans, P., Wilcox, J., Gopstein, A. M., Arent, D., Wofsy, S., Brown, N. J., Bradley, R., Stucky, G. D., Eardley, D., and Harriss, R.: Methane leaks from North American natural gas systems, Science, 343, 733-735, 10.1126/science.1247045, 2014.

Cambaliza, M., Shepson, P., Bogner, J., Caulton, D., Stirm, B., Sweeney, C., Montzka, S., Gurney, K., Spokas, K., and Salmon, O.: Quantification and source apportionment of the methane emission flux from the city of Indianapolis, Elem. Sci. Anth., 3, 2015.

Cambaliza, M. O. L., Shepson, P. B., Caulton, D. R., Stirm, B., Samarov, D., Gurney, K. R., Turnbull, J., Davis, K. J., Possolo, A., Karion, A., Sweeney, C., Moser, B., Hendricks, A., Lauvaux, T., Mays, K., Whetstone, J., Huang, J., Razlivanov, I., Miles, N. L., and Richardson, S. J.: Assessment of uncertainties of an aircraft-based mass balance approach for quantifying urban greenhouse gas emissions, Atmos. Chem. Phys., 14, 9029-9050, 10.5194/acp-14-9029-2014, 2014.

Carslaw, D. C., and Ropkins, K.: openair — An R package for air quality data analysis, Environmental Modelling & Software, 27-28, 52-61, https://doi.org/10.1016/j.envsoft.2011.09.008, 2012.

Carslaw, D. C., and Beevers, S. D.: Characterising and understanding emission sources using bivariate polar plots and k-means clustering, Environmental Modelling & Software, 40, 325-329, https://doi.org/10.1016/j.envsoft.2012.09.005, 2013.

Ciais, P., Sabine, C., Bala, G., Bopp, L., Brovkin, V., Canadell, J., Chhabra, A., DeFries, R., Galloway, J., and Heimann, M.: Carbon and other biogeochemical cycles, in: Working Group I Contribution To The IPCC Fifth Assessment Report. Climate Change 2013 - The Physical Science Basis, edited by: Stocker, T. F., Qin, D., Plattner, G., Tignor, M., Allen,

S., Boschung, J., Nauels, A., Xia, Y., Bex, V., and Midgley, P., Cambridge Univ. Press, 465-570, 2013.

Davis, K. J., Deng, A., Lauvaux, T., Miles, N. L., Richardson, S. J., Sarmiento, D. P., Gurney, K. R., Hardesty, R. M., Bonin, T. A., and Brewer, W. A.: The Indianapolis Flux Experiment (INFLUX): A test-bed for developing urban greenhouse gas emission measurements, Elem. Sci. Anth., 5, 2017.

Deng, A., Lauvaux, T., Davis, K. J., Gaudet, B. J., Miles, N., Richardson, S. J., Wu, K., Sarmiento, D. P., Hardesty, R. M., and Bonin, T. A.: Toward reduced transport errors in a high resolution urban CO_2 inversion system, Elem. Sci. Anth., 5, 2017.

Efron, B., and Tibshirani, R.: Bootstrap methods for standard errors, confidence intervals, and other measures of statistical accuracy, Statist. Sci., 1, 54-75, 10.1214/ss/1177013815, 1986.

European Commission Joint Research Centre, Netherlands Environmental Assessment Agency: Emission Database for Global Atmospheric Research (EDGAR), Release Version 4.2, available at: http://edgar.jrc.ec.europa.eu, 2010.

Gurney, K. R., Razlivanov, I., Song, Y., Zhou, Y., Benes, B., and Abdul-Massih, M.: Quantification of fossil fuel CO_2 emissions on the building/street scale for a large U.S. city, Environmental Science & Technology, 46, 12194-12202, 10.1021/es3011282, 2012.

Hanna, S. R., Briggs, G. A., and Hosker Jr, R. P.: Handbook on atmospheric diffusion, National Oceanic and Atmospheric Administration, Oak Ridge, TN (USA). Atmospheric Turbulence and Diffusion Lab., 1982.

Heimburger, A. M., Harvey, R. M., Shepson, P. B., Stirm, B. H., Gore, C., Turnbull, J., Cambaliza, M. O., Salmon, O. E., Kerlo, A.-E. M., and Lavoie, T. N.: Assessing the optimized precision of the aircraft mass balance method for measurement of urban greenhouse gas emission rates through averaging, Elem. Sci. Anth., 5, 2017.

Helfter, C., Tremper, A. H., Halios, C. H., Kotthaus, S., Bjorkegren, A., Grimmond, C. S. B., Barlow, J. F., and Nemitz, E.: Spatial and temporal variability of urban fluxes of methane, carbon monoxide and carbon dioxide above London, UK, Atmos. Chem. Phys., 16, 10543-10557, 10.5194/acp-16-10543-2016, 2016.

Hendrick, M. F., Ackley, R., Sanaie-Movahed, B., Tang, X., and Phillips, N. G.: Fugitive methane emissions from leak-prone natural gas distribution infrastructure in urban

690 environments, Environmental Pollution, 213, 710-716,
691 https://doi.org/10.1016/j.envpol.2016.01.094, 2016.
692 Hiller, R. V., Neininger, B., Brunner, D., Gerbig, C., Bretscher, D., Künzle, T., Buchmann, N.,
693 and Eugster, W.: Aircraft-based CH_4 flux estimates for validation of emissions from an
694 agriculturally dominated area in Switzerland, Journal of Geophysical Research:
695 Atmospheres, 119, 4874-4887, doi:10.1002/2013JD020918, 2014.
696 Hmiel, B., Petrenko, V. V., Dyonisius, M. N., Buizer, C., Smith A. M., Place, P. F., Harth, C.,
697 Beaudette, R., Hua, Q., Yang, B., Vimont, I., Michel, S. E., Severinghaus, J. P.,
698 Etheridge, D., Bromley, Schmitt, J., Faïn, X., Weiss, R. F., and Dlugokencky, E.:
699 Preindustrial $^{14}CH_4$ indicates greater anthropogenic fossil CH_4 emissions, Nature, 578,
700 409–412, https://doi.org/10.1038/s41586-020-1991-8, 2020.
701 Jackson, R. B., Down, A., Phillips, N. G., Ackley, R. C., Cook, C.W., Plata, D. L., and Zhao, K.
702 G.: Natural gas pipeline leaks across Washington, DC, Environ. Sci. Technol., 48, 2051–
703 2058, doi:10.1021/es404474x, 2014.
704 Jeong, S., Millstein, D., and Fischer, M. L.: Spatially explicit methane emissions from petroleum
705 production and the natural gas system in California, Environmental Science &
706 Technology, 48, 5982-5990, 10.1021/es4046692, 2014.
707 Jeong, S., Newman, S., Zhang, J., Andrews, A. E., Bianco, L., Bagley, J., Cui, X., Graven, H.,
708 Kim, J., Salameh, P., LaFranchi, B. W., Priest, C., Campos-Pineda, M., Novakovskaia,
709 E., Sloop, C. D., Michelsen, H. A., Bambha, R. P., Weiss, R. F., Keeling, R., and Fischer,
710 M. L.: Estimating methane emissions in California's urban and rural regions using
711 multitower observations, Journal of Geophysical Research: Atmospheres, 121, 13,031-
712 013,049, doi:10.1002/2016JD025404, 2016.
713 Jeong, S., Cui, X., Blake, D. R., Miller, B., Montzka, S. A., Andrews, A., Guha, A., Martien, P.,
714 Bambha, R. P., LaFranchi, B., Michelsen, H. A., Clements, C. B., Glaize, P., and Fischer,
715 M. L.: Estimating methane emissions from biological and fossil-fuel sources in the San
716 Francisco Bay Area, Geophysical Research Letters, 44, 486-495,
717 doi:10.1002/2016GL071794, 2017.
718 Karion, A., Sweeney, C., Kort, E. A., Shepson, P. B., Brewer, A., Cambaliza, M., Conley, S. A.,
719 Davis, K., Deng, A., Hardesty, M., Herndon, S. C., Lauvaux, T., Lavoie, T., Lyon, D.,
720 Newberger, T., Pétron, G., Rella, C., Smith, M., Wolter, S., Yacovitch, T. I., and Tans,

P.: Aircraft-based estimate of total methane emissions from the Barnett Shale region, Environ. Sci. Technol., 49, 8124–8131, doi:10.1021/acs.est.5b00217, 2015

Kort, E. A., Eluszkiewicz, J., Stephens, B. B., Miller, J. B., Gerbig, C., Nehrkorn, T., Daube, B. C., Kaplan, J. O., Houweling, S., and Wofsy, S. C.: Emissions of CH_4 and N_2O over the United States and Canada based on a receptor-oriented modeling framework and COBRA-NA atmospheric observations, Geophys. Res. Lett., 35, L18808, doi:10.1029/2008GL034031, 2008.

Lamb, B. K., Cambaliza, M. O. L., Davis, K. J., Edburg, S. L., Ferrara, T. W., Floerchinger, C., Heimburger, A. M. F., Herndon, S., Lauvaux, T., Lavoie, T., Lyon, D. R., Miles, N., Prasad, K. R., Richardson, S., Roscioli, J. R., Salmon, O. E., Shepson, P. B., Stirm, B. H., and Whetstone, J.: Direct and indirect measurements and modeling of methane emissions in Indianapolis, Indiana, Environmental Science & Technology, 50, 8910-8917, 10.1021/acs.est.6b01198, 2016.

Lauvaux, T., Miles, N. L., Deng, A., Richardson, S. J., Cambaliza, M. O., Davis, K. J., Gaudet, B., Gurney, K. R., Huang, J., O'Keefe, D., Song, Y., Karion, A., Oda, T., Patarasuk, R., Razlivanov, I., Sarmiento, D., Shepson, P., Sweeney, C., Turnbull, J., and Wu, K.: High-resolution atmospheric inversion of urban CO_2 emissions during the dormant season of the Indianapolis Flux Experiment (INFLUX), Journal of Geophysical Research: Atmospheres, 121, 5213-5236, doi:10.1002/2015JD024473, 2016.

Maasakkers, J. D., Jacob, D. J., Sulprizio, M. P., Turner, A. J., Weitz, M., Wirth, T., Hight, C., DeFigueiredo, M., Desai, M., Schmeltz, R., Hockstad, L., Bloom, A. A., Bowman, K. W., Jeong, S., and Fischer, M. L.: Gridded national inventory of U.S. methane emissions, Environmental Science & Technology, 50, 13123-13133, 10.1021/acs.est.6b02878, 2016.

Mays, K. L., Shepson, P. B., Stirm, B. H., Karion, A., Sweeney, C., and Gurney, K. R.: Aircraft-based measurements of the carbon footprint of Indianapolis, Environmental Science & Technology, 43, 7816-7823, 10.1021/es901326b, 2009.

McKain, K., Down, A., Raciti, S. M., Budney, J., Hutyra, L. R., Floerchinger, C., Herndon, S. C., Nehrkorn, T., Zahniser, M. S., Jackson, R. B., Phillips, N., and Wofsy, S. C.: Methane emissions from natural gas infrastructure and use in the urban region of Boston, Massachusetts, Proceedings of the National Academy of Sciences, 112, 1941-1946, 10.1073/pnas.1416261112, 2015.

Miles, N. L., Richardson, S. J., Lauvaux, T., Davis, K. J., Balashov, N. V., Deng, A., Turnbull, J. C., Sweeney, C., Gurney, K. R., and Patarasuk, R.: Quantification of urban atmospheric boundary layer greenhouse gas dry mole fraction enhancements in the dormant season: Results from the Indianapolis Flux Experiment (INFLUX), Elem. Sci. Anth., 5, 2017.

Miller, S. M., Wofsy, S. C., Michalak, A. M., Kort, E. A., Andrews, A. E., Biraud, S. C., Dlugokencky, E. J., Eluszkiewicz, J., Fischer, M. L., Janssens-Maenhout, G., Miller, B. R., Miller, J. B., Montzka, S. A., Nehrkorn, T., and Sweeney, C.: Anthropogenic emissions of methane in the United States, Proceedings of the National Academy of Sciences, 110, 20018-20022, 10.1073/pnas.1314392110, 2013.

Myhre, G., Shindell, D., Bréon, F. M., Collins, W., Fuglestvedt, J., Huang, J., Koch, D., Lamarque, J. F., Lee, D., Mendoza, B., Nakajima, T., Robock, A., Stephens, G., Takemura, T., and Zhang, H.: Anthropogenic and natural radiative forcing, in: Climate Change 2013: The Physical Science Basis. Contribution of Working Group I to the Fifth Assessment Report of the Intergovernmental Panel on Climate Change, edited by: Stocker, T. F., Qin, D., Plattner, G. K., Tignor, M., Allen, S. K., Doschung, J., Nauels, A., Xia, Y., Bex, V., and Midgley, P. M., Cambridge University Press, Cambridge, UK, 659-740, 2013.

National Academies of Sciences and Medicine: Improving characterization of anthropogenic methane emissions in the United States, The National Academies Press, Washington, DC, 250 pp., 2018.

Nisbet, E. G., Dlugokencky, E. J., Manning, M. R., Lowry, D., Fisher, R. E., France, J. L., Michel, S. E., Miller, J. B., White, J. W. C., Vaughn, B., Bousquet, P., Pyle, J. A., Warwick, N. J., Cain, M., Brownlow, R., Zazzeri, G., Lanoisellé, M., Manning, A. C., Gloor, E., Worthy, D. E. J., Brunke, E.-G., Labuschagne, C., Wolff, E. W., and Ganesan, A. L.: Rising atmospheric methane: 2007–2014 growth and isotopic shift, Global Biogeochemical Cycles, 30, 1356-1370, doi:10.1002/2016GB005406, 2016.

Nisbet, E. G., Manning, M. R., Dlugokencky, E. J., Fisher, R. E., Lowry, D., Michel, S. E., Myhre, C. L., Platt, S. M., Allen, G., Bousquet, 15 P., Brownlow, R., Cain, M., France, J. L., Hermansen, O., Hossaini, R., Jones, A. E., Levin, I., Manning, A. C., Myhre, G., Pyle, J. A., Vaughn, B. H., Warwick, N. J., and White, J. W. C.: Very Strong Atmospheric Methane Growth in the 4 Years 2014–2017: Implications for the Paris Agreement, Global

Biogeochemical Cycles, 33, 318–342, https://doi.org/10.1029/2018GB006009, https://agupubs.onlinelibrary. wiley.com/doi/abs/10.1029/2018GB006009, 2019.

Richardson, S. J., Miles, N. L., Davis, K. J., Lauvaux, T., Martins, D. K., Turnbull, J. C., McKain, K., Sweeney, C., and Cambaliza, M. O. L.: Tower measurement network of in-situ CO_2, CH_4, and CO in support of the Indianapolis FLUX (INFLUX) Experiment, Elem Sci Anth, 5, 2017.

Sarmiento, D. P., Davis, K. J., Deng, A., Lauvaux, T., Brewer, A., and Hardesty, M.: A comprehensive assessment of land surface-atmosphere interactions in a WRF/Urban modeling system for Indianapolis, IN, Elem. Sci. Anth., 5, 2017.

Saunois, M., Jackson, R. B., Bousquet, P., Poulter, B., and Canadell, J. G.: The growing role of methane in anthropogenic climate change, Environmental Research Letters, 11, 120207, 2016.

Schuh, A. E., Lauvaux, T., West, T. O., Denning, A. S., Davis, K. J., Miles, N., Richardson, S., Uliasz, M., Lokupitiya, E., Cooley, D., Andrews, A., and Ogle, S.: Evaluating atmospheric CO_2 inversions at multiple scales over a highly inventoried agricultural landscape, Global change biology, 19, 1424-1439, doi:10.1111/gcb.12141, 2013.

Taylor, D. M., Chow, F. K., Delkash, M., and Imhoff, P. T.: Atmospheric modeling to assess wind dependence in tracer dilution method measurements of landfill methane emissions, Waste Management, 73, 197-209, https://doi.org/10.1016/j.wasman.2017.10.036, 2018.

Townsend-Small, A., Tyler, S. C., Pataki, D. E., Xu, X., and Christensen, L. E.: Isotopic measurements of atmospheric methane in Los Angeles, California, USA: Influence of "fugitive" fossil fuel emissions, J. Geophys. Res.-Atmos., 117, 1–11, https://doi.org/10.1029/2011JD016826, 2012.

Turnbull, J. C., Sweeney, C., Karion, A., Newberger, T., Lehman, S. J., Tans, P. P., Davis, K. J., Lauvaux, T., Miles, N. L., Richardson, S. J., Cambaliza, M. O., Shepson, P. B., Gurney, K., Patarasuk, R., and Razlivanov, I.: Toward quantification and source sector identification of fossil fuel CO_2 emissions from an urban area: Results from the INFLUX experiment, Journal of Geophysical Research: Atmospheres, 120, 292-312, doi:10.1002/2014JD022555, 2015.

Turnbull, J. C., Karion, A., Davis, K. J., Lauvaux, T., Miles, N. L., Richardson, S. J., Sweeney, C., McKain K., Lehman, S. J., Gurney, K., Patarasuk, R., Jianming L., Shepson, P. B.,

Heimburger A., Harvey, R., and Whetstone, J.: Synthesis of urban CO_2 emission estimates from multiple methods from the Indianapolis Flux Project (INFLUX), Environmental Science and Technology, 53 (1), 287-295, 10.1021/acs.est.8b05552, 2019.

U.S. Environmental Protection Agency: Inventory of U.S. Greenhouse Gas Emissions and Sinks: 1990–2011, Technical Report EPA 430-R-13-001, Environmental Protection Agency, Washington, 505 pp., 2013.

Van De Wiel, B. J. H. V. d., Moene, A. F., Jonker, H. J. J., Baas, P., Basu, S., Donda, J. M. M., Sun, J., and Holtslag, A. A. M.: The minimum wind speed for sustainable turbulence in the nocturnal boundary layer, Journal of the Atmospheric Sciences, 69, 3116-3127, 10.1175/jas-d-12-0107.1, 2012.

Wunch, D., Wennberg, P. O., Toon, G. C., Keppel-Aleks, G., and Yavin, Y. G.: Emissions of greenhouse gases from a North American megacity, Geophysical Research Letters, 36, doi:10.1029/2009GL039825, 2009.

Zavala-Araiza, D., Lyon, D. R., Alvarez, R. A., Davis, K. J., Harriss, R., Herndon, S. C., Karion, A., Kort, E. A., Lamb, B. K., Lan, X., Marchese, A. J., Pacala, S. W., Robinson, A. L., Shepson, P. B., Sweeney, C., Talbot, R., Townsend-Small, A., Yacovitch, T. I., Zimmerle, D. J., and Hamburg, S. P.: Reconciling divergent estimates of oil and gas methane emissions, Proceedings of the National Academy of Sciences, 112, 15597-15602, 10.1073/pnas.1522126112, 2015.

Tables

Table 1. INFLUX towers used to estimate CH_4 background based on two different criteria. Numbers in bold indicate towers chosen to generate a background field when multiple options are possible (for more details see discussion). In short, criterion 1 uses towers with the lowest mean CH_4 for a specific wind direction, and criterion 2 uses towers outside of Marion County and not downwind of large sources (including the city as a whole).

Wind Direction	CH_4 Background Towers	
	Criterion 1	Criterion 2
North (N)	8	**13**, 8
Northeast (NE)	8	**13**, 8, 2
East (E)	**2**, 8	**8**, 4, 1, 2
Southeast (SE)	1	**8**, 13, 4, 1
South (S)	1	**4**, 13, 1
Southwest (SW)	13	**1**, 4
West (W)	1	**4**, 1
Northwest (NW)	1	**8**, 1

Table 2. A number of independent samples needed (column 4) to satisfy combined requirement of 6 ppb background error based on the sum of bias and random error (explained in section 3.2) as a function of wind direction.

Wind Direction	Bias (ppb)	Threshold (ppb)	Samples Needed
N	1	5	74
NE	1	5	36
E	0.5	5.5	46
SE	4	2	>150
S	2	4	53
SW	4.5	1.5	>150
W	3	3	52
NW	5	1	>150

Figures

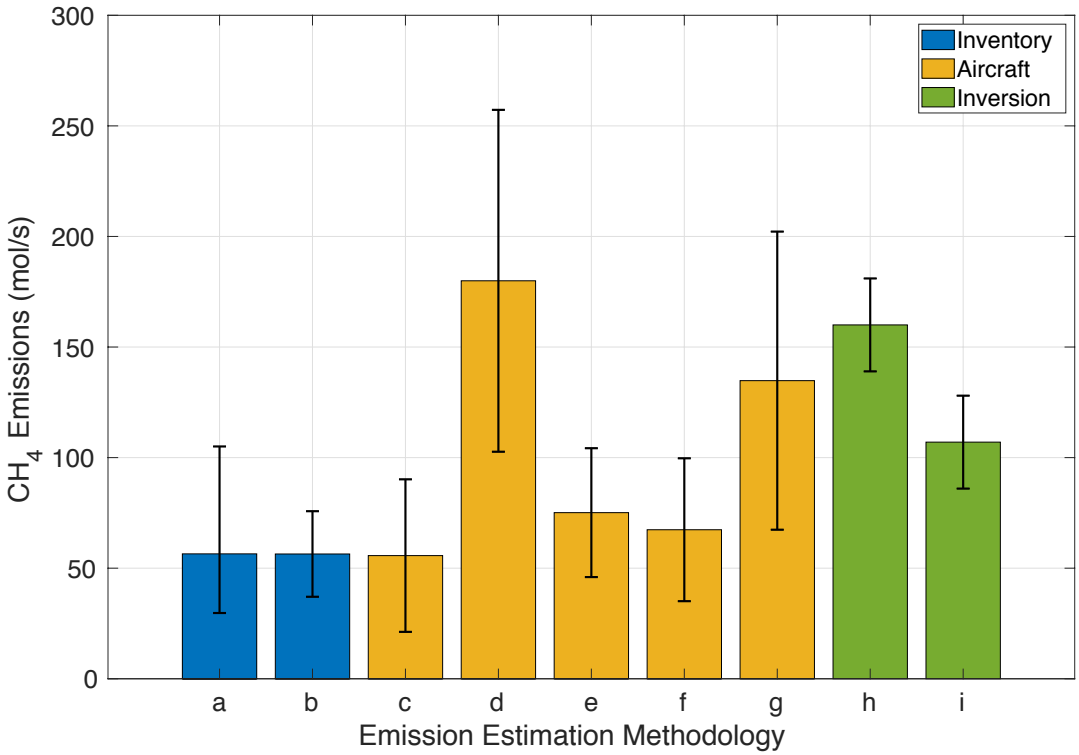

Figure 1. Various estimates of CH_4 emissions at Indianapolis. **(a, b)** Bottom-up estimates of CH_4 emissions conducted by Lamb et al. (2016) in 2013 and Maasakkers et al. (2016) based on the EPA 2012 inventory respectively. Error bars show 95% confidence intervals (for more details see above-mentioned articles). **(c-g)** Top-down evaluations of CH_4 emissions with aircraft from various flight campaigns where **(c)** contains 5 flights over March-April of 2008, **(d)** contains 3 flights over November-January of 2008-09, **(e)** contains 5 flights over April-July of 2011, **(f)** contains 9 flights from November-December, 2014, and **(g)** contains the same 5 flights over April-July of 2011 as in (e) but uses different methodology. Methodologies for **(c-f)** are described in Lamb et al. (2016) and methodology for **(g)** is described in Cambaliza et al. (2015). Error bars show 95% confidence intervals (for more details see above-mentioned articles). **(h, i)** Top-down evaluations of CH_4 emissions for 2012-2013 using tower inversion

modeling methodology with two different domains, where **(h)** uses the full domain of Figure 2 and **(i)** uses only the Marion County domain of Figure 2. The inversion methodology and 95% confidence intervals are described in detail in Lamb et al. (2016).

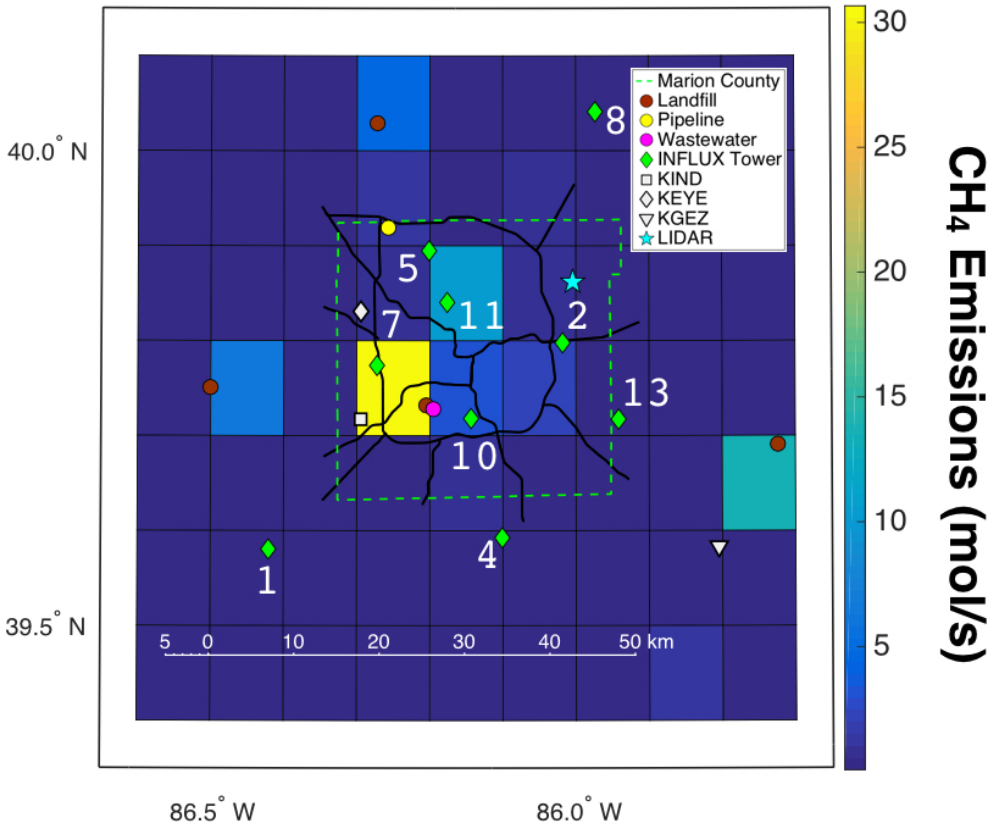

Figure 2. Map of the primary roads in Indianapolis, INFLUX towers, lidar system, weather stations, and a few CH_4 point sources plotted over the gridded CH_4 emissions (mol/s) from the EPA 2012 Inventory (Maasakkers et al., 2016). The gridded map of emissions includes emissions from the mentioned point sources; their position is provided to aid in interpretation of the observations. The dashed bright green line denotes Marion County borders.

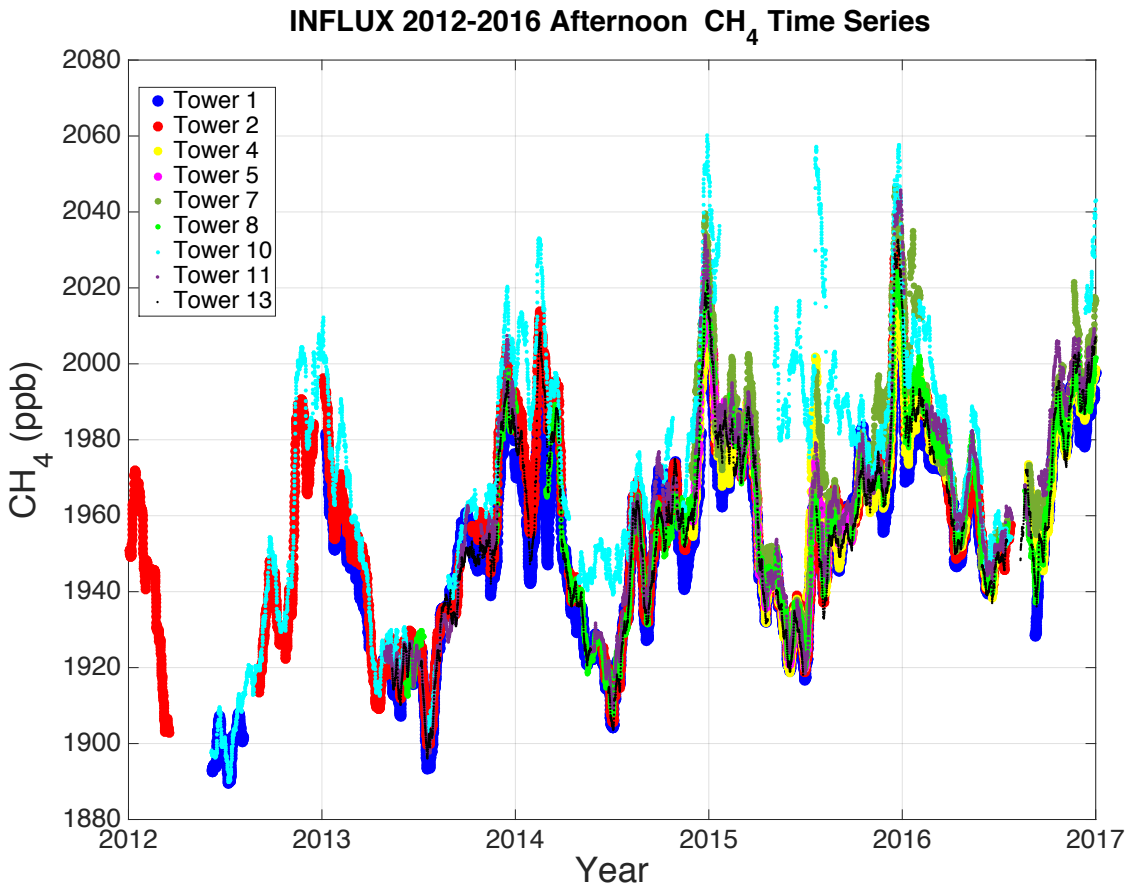

946

947 **Figure 3.** 20-day running average of afternoon (12-16 LST; the hours are inclusive) CH_4 mole fractions
948 as measured by the INFLUX tower network (highest available height is used) from 2012 through 2016.

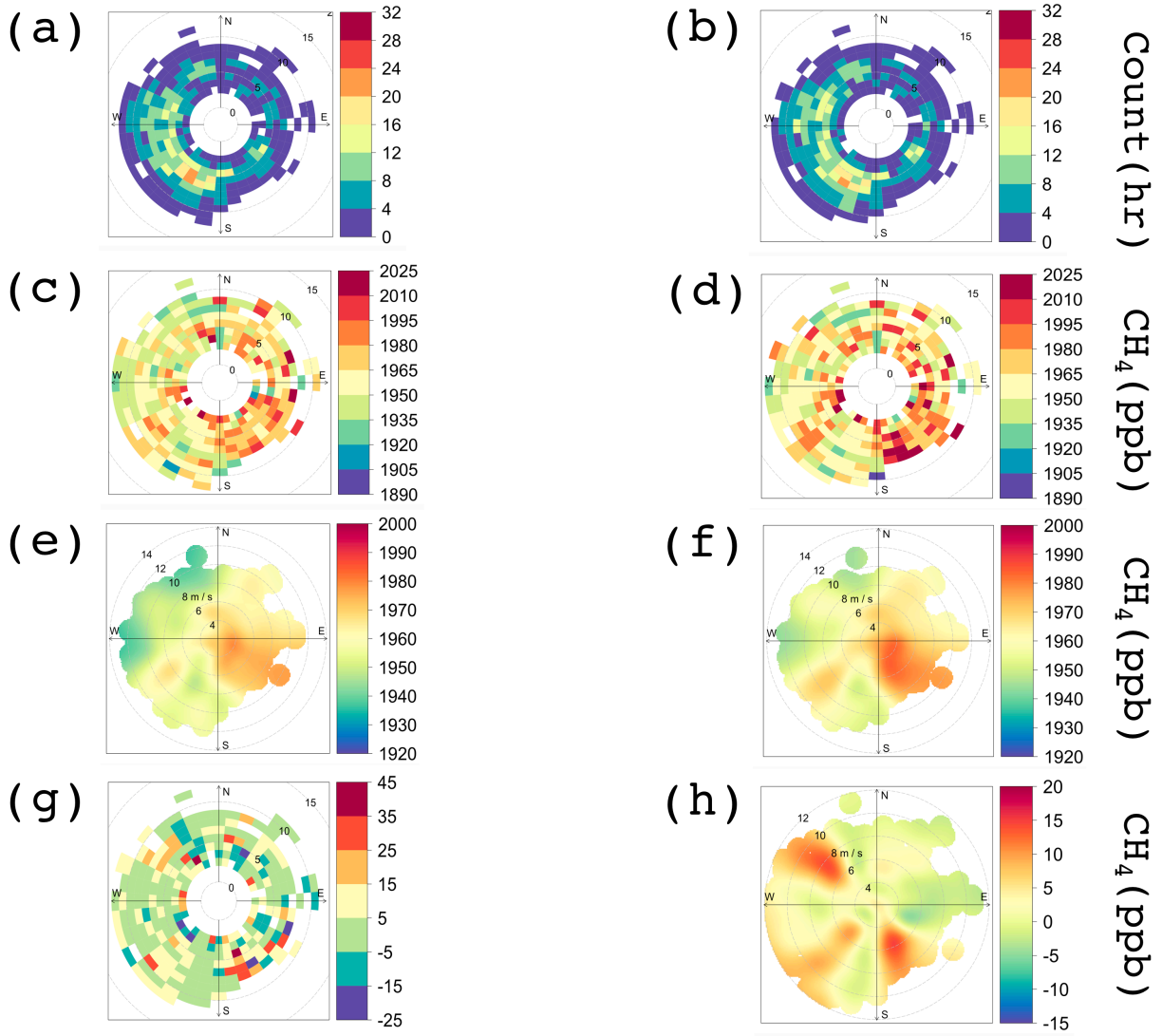

Figure 4. Frequency and bivariate polar plots of CH_4 background for Indianapolis using data from 12-16 LST, November 2014 through December 2016 given 2 different criteria (Table 1). **(a)** Polar histogram indicating a number of hourly measurements available using criterion 1. **(b)** Same as (a) only for criterion 2. Differences between (a) and (b) are due to slight differences in data availability at the considered towers. **(c)** Polar frequency plot of the CH_4 background using criterion 1. **(d)** Same as (c) only for criterion 2. **(e)** Polar bivariate plot of CH_4 background using criterion 1. **(f)** Same as (e) only for criterion 2. **(g)** Polar frequency plot of difference between the backgrounds: $criterion\ 2 - criterion\ 1$. **(h)** Same as (g) but shown with a bivariate polar plot.

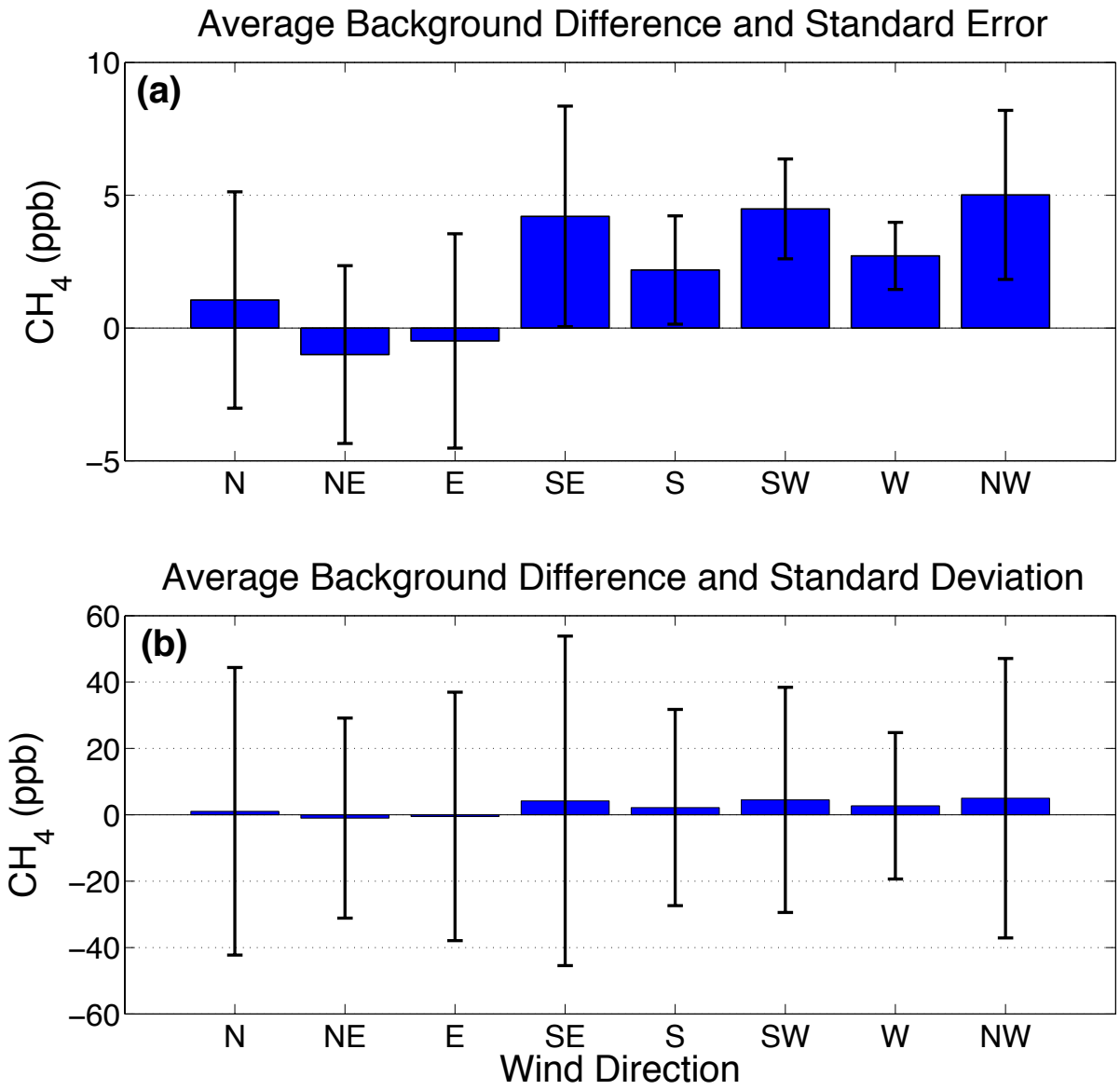

959
960 **Figure 5.** Average of the differences between criteria 2 and 1 CH_4 backgrounds at Indianapolis as a
961 function of wind direction. These averages are generated from the same data that is used in Figure 4 and
962 reflect results shown in Figure 4g. Error bars indicate in **(a)** 2 × standard error and in **(b)** 2 × standard
963 deviation.

964

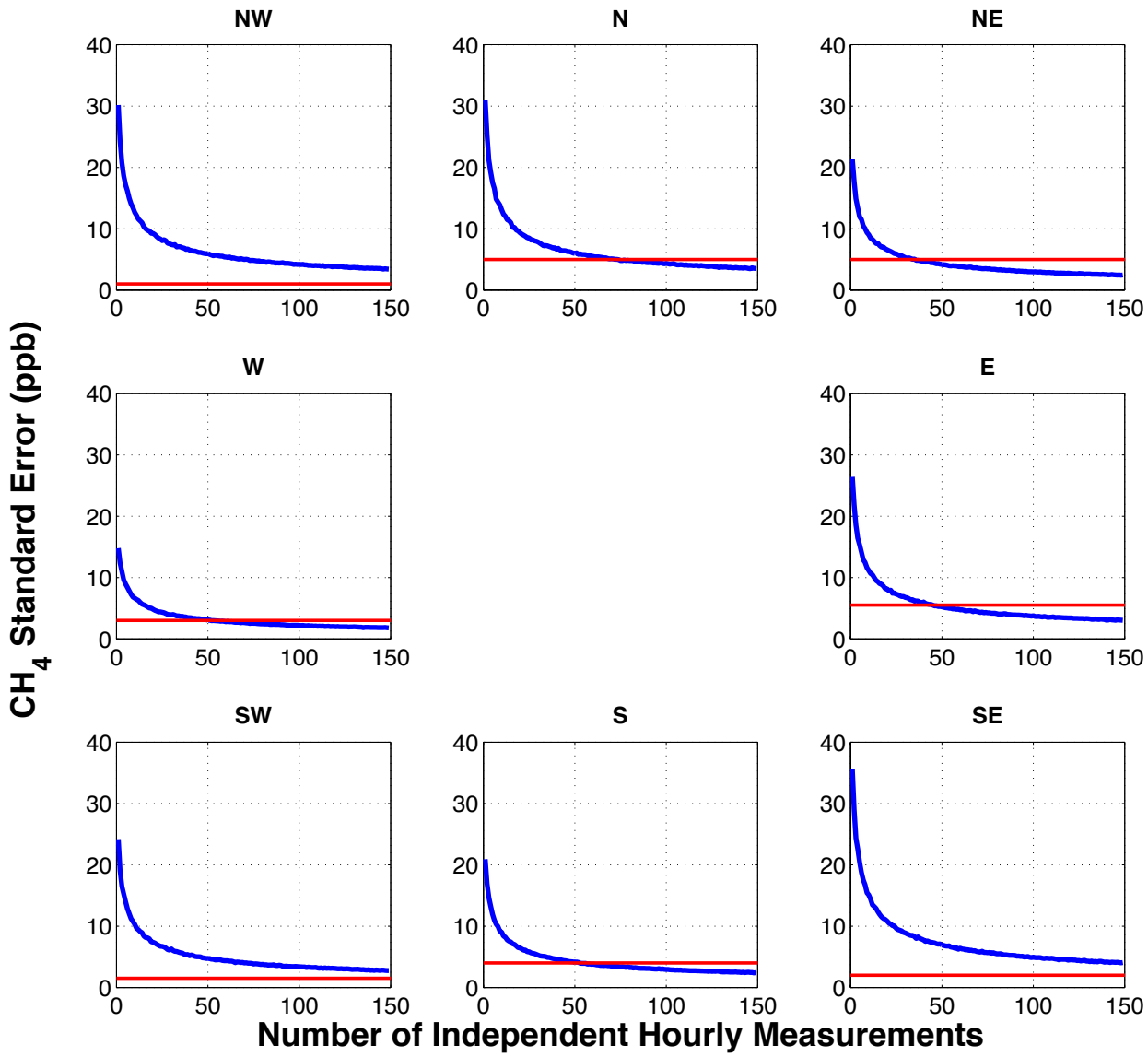

Figure 6. Bootstrap simulation of the standard errors × 2 in Indianapolis CH_4 background mole fraction differences (between criteria 2 and 1) as a function of sample size and wind direction (see text for details). Thresholds for each of the wind directions indicate a random error threshold needed for the background uncertainty to be within 50% of Indianapolis CH_4 enhancement of 12 ppb.

970

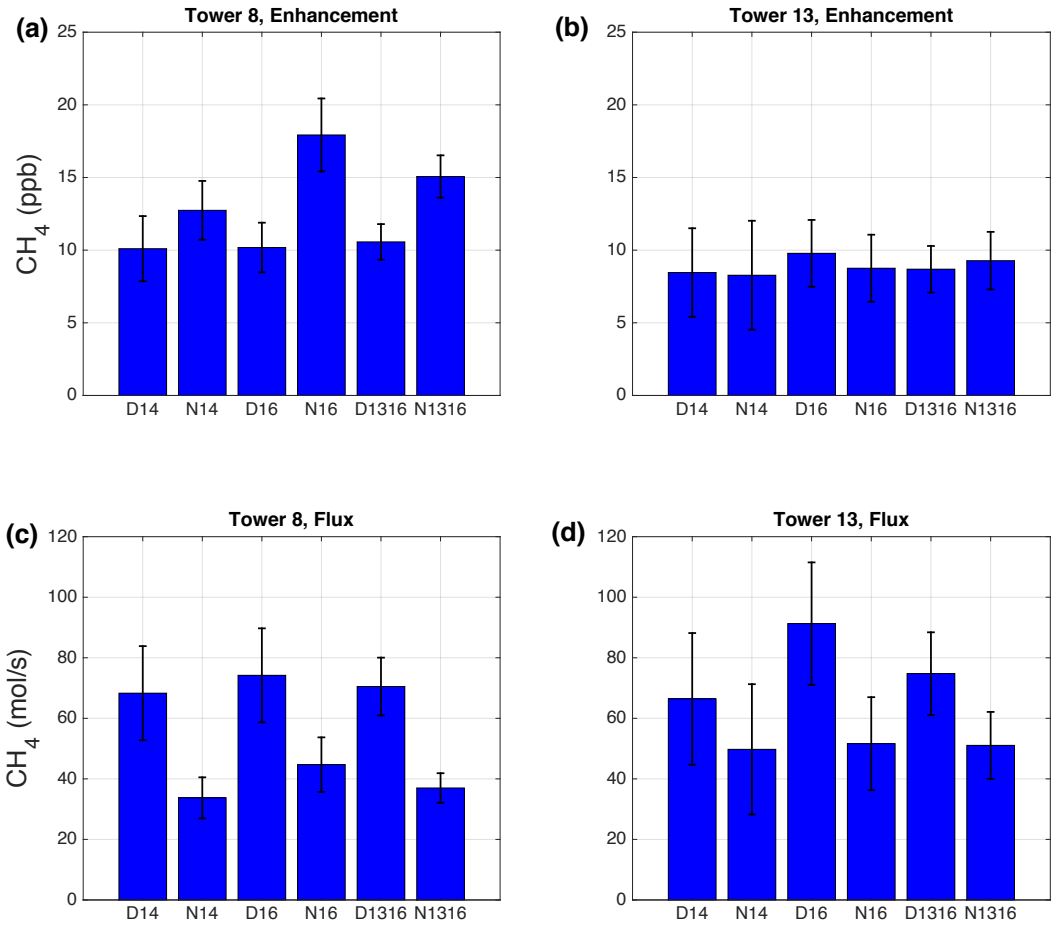

971

972 **Figure 7.** Averages of the daytime (D) and nighttime (N) CH_4 enhancements and fluxes at INFLUX
973 towers 8 and 13 for years 2014 (14), 2016 (16), and 2013-2016 (1316). The error bars represent 95%
974 confidence interval of each mean value. **(a)** Estimates of CH_4 enhancements from tower 8. **(b)** Estimates
975 of CH_4 enhancements from tower 13. **(c)** Estimates of CH_4 flux from tower 8. **(d)** Estimates of CH_4 flux
976 from tower 13.

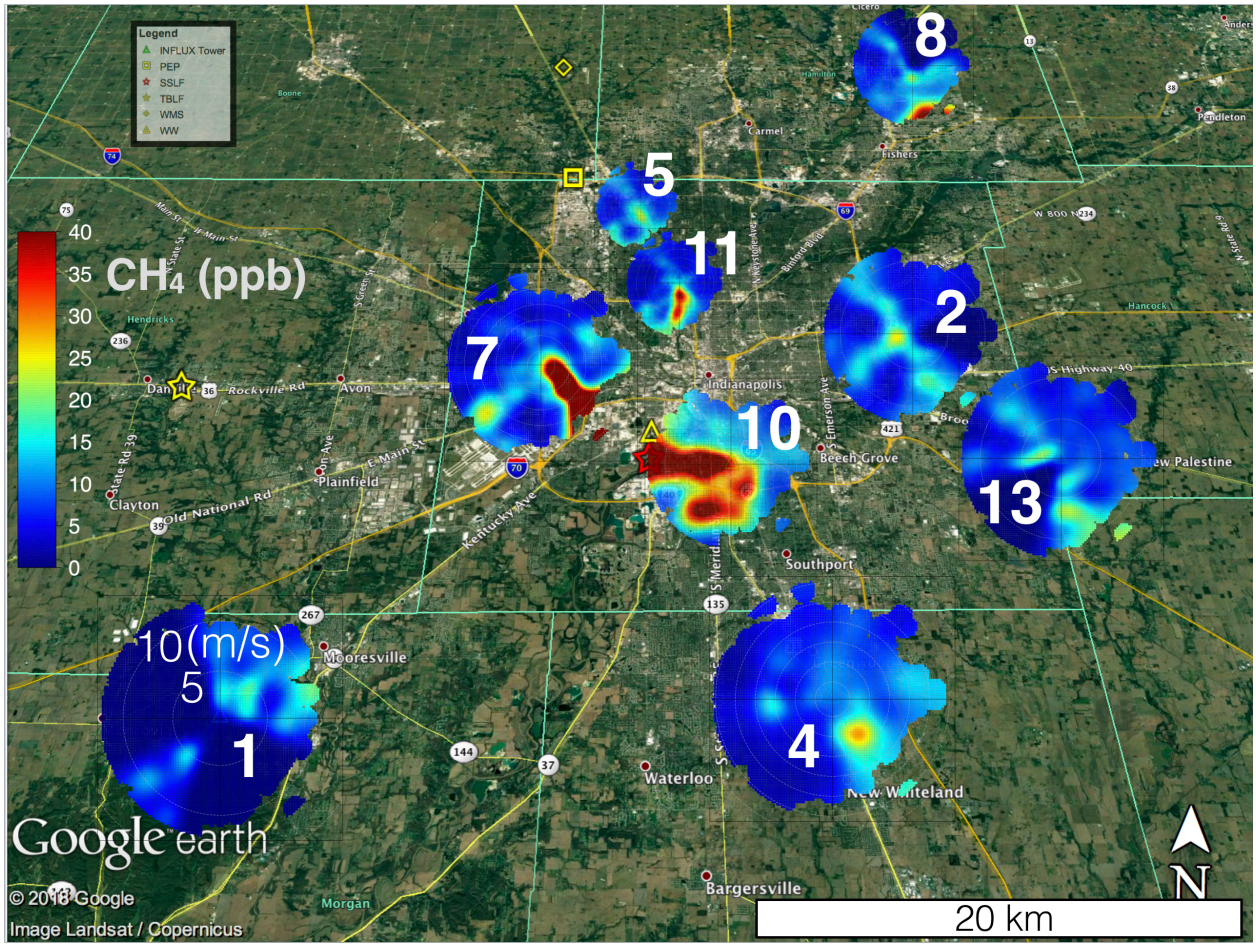

977
978 **Figure 8.** Google Earth image overlaid with bivariate polar plots (section 2.5) of the CH_4 enhancements
979 at 9 INFLUX towers in Indianapolis using the criterion 1 background (Table 1) for full years of 2014 and
980 2015 over the afternoon (12-16 LST). The wind speed scale is only labeled at site 1; other sites follow
981 the same convention. Legend indicates known sources of CH_4: Panhandle Eastern Pipeline (PEP),
982 Southern Side Landfill (SSLF), Twin Bridges Landfill (TBLF), Waste Management Solutions (WMS),
983 and Waste Water treatment facility (WW). The known magnitudes of sources that are in Marion County
984 (PEP, SSLF, and WW) are reported in section 2.7. Magnitudes of TBLF and WMS according to EPA are
985 approximately 5 mol/s. The largest known source on the map is SSLF.

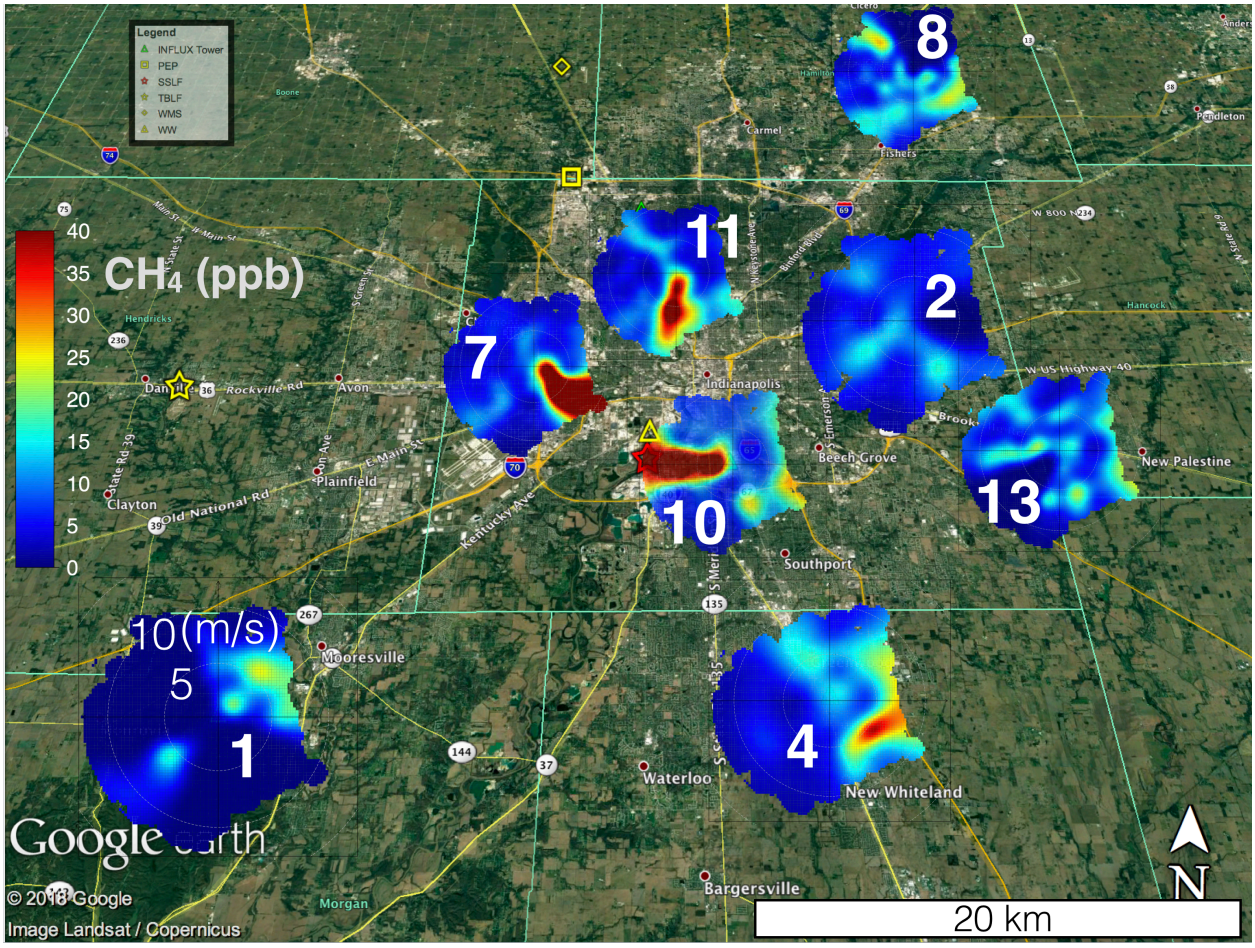

Figure 9. Google Earth image overlaid with bivariate polar plots (section 2.5) of the CH_4 enhancements at 9 INFLUX towers in Indianapolis using the criterion 1 background (Table 1) for year 2016 over the afternoon (12-16 LST). The wind speed scale is only labeled at site 1; other sites follow the same convention. Legend indicates known sources of CH_4: Panhandle Eastern Pipeline (PEP), Southern Side Landfill (SSLF), Twin Bridges Landfill (TBLF), Waste Management Solutions (WMS), and Waste Water treatment facility (WW). The known magnitudes of sources that are in Marion County (PEP, SSLF, and WW) are reported in section 2.7. Magnitudes of TBLF and WMS according to EPA are approximately 5 mol/s. The largest known source on the map is SSLF.